


Article

Detailed Trend Analysis of Extreme Climate Indices in the Upper Geum River Basin

Micah Lourdes Felix ¹, Young-kyu Kim ^{1,*}, Mikyoung Choi ², Joo-Cheol Kim ², Xuan Khanh Do ³, Thu Hien Nguyen ³ and Kwansue Jung ¹

¹ Department of Civil Engineering, Chungnam National University, Daejeon 305-764, Korea; mafelix.cnu@gmail.com (M.L.F.); ksjung@cnu.ac.kr (K.J.)

² International Water Resources Research Institute, Daejeon 305-764, Korea; choi.mk1981@gmail.com (M.C.); kjoocheol@hanmail.net (J.-C.K.)

³ Faculty of Water Resources Engineering, Thuyloi University, Hanoi 115000, Vietnam; kxanh.thuyluc@tlu.edu.vn (X.K.D.); hien@tlu.edu.vn (T.H.N.)

* Correspondence: youngkim6257@gmail.com

Abstract: To investigate the recent effects of climate change in the upper Geum River basin in South Korea, a detailed trend analysis of 17 extreme climate indices based on 33 years (1988–2020) of daily precipitation, and daily (minimum and maximum) temperature data has been analyzed in this study. Out of the 17 extreme climate indices, nine (eight) indices were based on temperature (precipitation) data. Trend analysis based on detailed temporal scales (annual, seasonal, monthly) were performed through the Mann–Kendall trend test and the Theil–Sen slope method. Furthermore, the Mann–Whitney–Pettit test was also applied in this study, to detect abrupt changes in the extreme climate indices. Based on the results of this study, the climate conditions at the upper Geum River basin for the past three decades can be summarized as follows: general increase in temperature intensity, decrease in cold duration, increased heat duration, increased precipitation intensity, and increased consecutive wet and dry durations. Furthermore, a prolonged summer season (shorter spring, and autumn periods) and precipitation shifts, were detected based on trend analysis results of seasonal, and monthly time scales. The results presented in this study can provide supplementary data for improving watershed management strategies in the upper Geum River basin.

Keywords: extreme climate index; Yongdam dam; trend analysis; Mann–Kendall; ETCCDI



Citation: Felix, M.L.; Kim, Y.-k.; Choi, M.; Kim, J.-C.; Do, X.K.; Nguyen, T.H.; Jung, K. Detailed Trend Analysis of Extreme Climate Indices in the Upper Geum River Basin. *Water* **2021**, *13*, 3171. <https://doi.org/10.3390/w13223171>

Academic Editor: Momcilo Markus

Received: 7 October 2021

Accepted: 8 November 2021

Published: 10 November 2021

Publisher's Note: MDPI stays neutral with regard to jurisdictional claims in published maps and institutional affiliations.



Copyright: © 2021 by the authors. Licensee MDPI, Basel, Switzerland. This article is an open access article distributed under the terms and conditions of the Creative Commons Attribution (CC BY) license (<https://creativecommons.org/licenses/by/4.0/>).

1. Introduction

Climate variability has been causing significant effects on the alternation of the hydro-climatic systems [1]. The frequent occurrence of unprecedented extreme weather events due to unpredictable climate, leads to human casualties, propriety, and economic losses. To better understand how a climate influences the frequency and intensity of extreme weather events, trends in the historical and future climate data have been widely investigated [2]. The Intergovernmental Panel on Climate Change (IPCC) [3] suggested that the characterization of both historical and future climate trends, to determine the effects of global warming on the frequency and intensity of extreme weather events, is crucial for assessing and developing strategies to minimize and regulate the impacts of climate change. In particular, trends in the temperature and precipitation are considered as two of the most important variables in understanding the climate, as the variation in these two climate variables can easily cause variation in the hydrological cycle [4]. While, the analysis of future climate trends is necessary for future climate risk assessments, the analysis of historical observed data plays a vital role in recognizing the current effects of global warming as compared from the past.

In terms of water resources, the trends of climate variables should be accurately analyzed for more efficient management of dam operations, such as maintaining efficient and safe

reservoir water levels, as preparation for unprecedented water-related disasters [5,6]. In year 2020, South Korea was heavily devastated with excessive precipitation during monsoon season (which is also locally known as 'Jangma' season, and henceforth called Jangma season), which brought 54 days of consecutive precipitation in the central part of the country, marking the highest record to date [7]. Due to these extreme events, the upper Geum River basin (UGRB) was brought with 378 mm of 2-day precipitation (highest record in 55 years), an increase of 40% of its previous of 270 mm (18–19 August 2004) [8]. As a result of the unpredicted extended Jangma season, Yongdam dam almost reached its full reservoir capacity at 98.9% (highest recorded data since year 2001), and had to release approximately 14.7% (approximately 119.94 M cubic meters; the highest record of released dam water) of its reservoir capacity on 8 August 2020; the sudden release of dam waters caused downstream flooding in the area. Therefore, to prevent future water-related disasters in a catchment, a detailed investigation of trends in climate variables should be performed.

A set of standard measurements of the extreme climate indices based daily precipitation, and daily (minimum and maximum) temperatures were provided by the Expert Team on Climate Change Detection and Indices (ETCCDI) [9,10]. For the past two decades, studies on trend analysis of ETCCDI indices [11–23], has been widely performed in different regions around the globe, through the use of Mann–Kendall (MK) trend test [24–26] and Theil–Sen (TS) slope estimator [27,28], both tests are rank-based non-parametric tests, that are insensitive to outliers and missing data. These recent studies were analyzed based on various temporal scales, ranging from annual [11–23], seasonal [13,17–19], and monthly [19] time scales. While, majority of the studies focused on annual scales, and lesser on monthly scales, the former is insufficient in providing detailed information in a watershed, such as detecting shifting of precipitation patterns. The studies of Ahmad et al. [29] and Azam et al. [30] proved that shifting in precipitation patterns can only be determined through trend analysis of precipitation based on monthly time scales. Therefore, the analysis of extreme climate indices based on annual, seasonal, and monthly time scales, are necessary to determine the detailed climate variability in a catchment.

In this study, the recent effects of climate change in the UGRB have been investigated through a detailed trend analysis of 17 extreme climate indices in the UGRB. The 17 core indices based on both precipitation and temperature data, were analyzed based on annual, seasonal, and monthly time scales. Furthermore, the two non-parametric trend tests, the Mann–Kendall trend test, and Theil–Sen slope estimator method, were used to detect and quantify the magnitude of trends in the time series. Moreover, the Mann–Whitney–Pettitt test, was also used to detect abrupt changes in the time series. Lastly, the correlation between trend magnitudes of all extreme climate indices, were also investigated in this study. The results provided in this study can be used to determine the vulnerability of the UGRB against the recent climate conditions.

2. Materials and Methods

2.1. Study Area

The Geum River basin, located at the central part of the country, as shown in Figure 1, is the third largest watershed next to Nakdong, and Han River basins. It has a catchment area of 9912 km², and the UGRB is situated at the most upstream part of the watershed, which constitutes 9.4% of Geum River basin. The UGRB is mostly characterized with mountainous topography, with elevations ranging from 204 m to 1608 m above sea level (a.s.l.). Furthermore, Yongdam dam, a concrete faced rock fill, multi-purpose dam is situated at the outlet of the UGRB, and was completed on year 2001. Its catchment area is approximately 930 km², with a reservoir area of 36.2 km², a storage capacity of 815 million m³ of water, and a flood control capacity of 137 million m³. Based on the 33 years (1988 to 2020) of daily climate data at Jangsu station, retrieved from the Korea Meteorological Agency (KMA), the catchment has an average annual precipitation of 1373.44 mm with an average number of 150 wet days, and an average temperature of 11.3 °C.

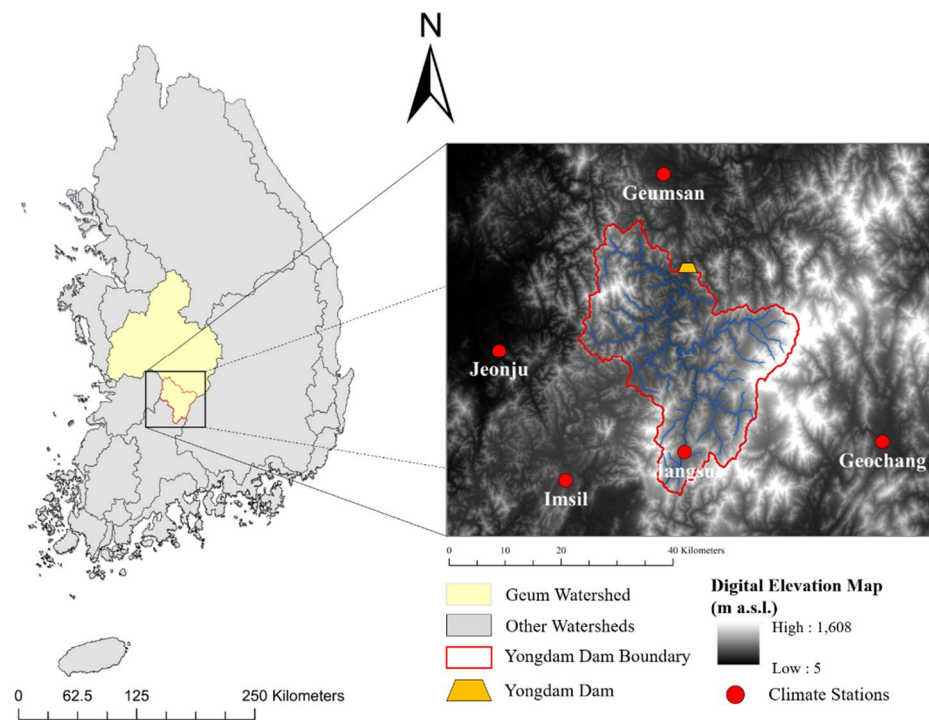


Figure 1. Location of the UGRB (red outline), Yongdam dam (orange trapezoid), and climate stations within Geum River basin (yellow) in South Korea.

In this study, the data from five climate stations near the UGRB (Figure 1) were analyzed. The detailed information for each climate station is summarized in Table 1. These five climate stations, all automated surface observing systems (ASOS), were selected due to their data reliability, with minimal missing data. In this study, the daily precipitation, daily minimum temperature, and daily maximum temperatures from year 1988 to 2020 (33 years), were used to calculate for the 17 extreme climate indices in the UGRB. The seasonal data for each station were calculated using daily data, and the following seasons considered in this study are: spring, (MAM), summer (JJA), autumn (SON), and winter (DJF).

Table 1. Detailed information for each climate station considered in this study.

No.	Station Name	Data Availability	Longitude (°E)	Latitude (°N)	Elevation (m. a.s.l.)
1	Jeonju	23 June 1918 to present 9 January	127.155	35.822	61.4
2	Geumsan	1972 to present	127.482	36.106	172.69
3	Imsil	2 June 1970 to present 1 January	127.286	35.612	247.04
4	Jangsu	1988 to present 24 January	127.520	35.657	406.49
5	Geochang	1972 to present	127.909	35.667	225.95

2.2. Extreme Climate Indices

The 17 extreme climate indices analyzed in this study, are summarized in Table 2. Nine and eight of the indices were derived from daily (maximum and minimum) temperature indices (No. 1–9), and daily precipitation indices (No. 10–17), respectively. While a majority

of the indices were analyzed based on three different temporal scales (i.e., annual, seasonal, and monthly), four indices (i.e., RX5 day, SDII, CDD, and CWD) were only analyzed based on an annual time scale. These four indices produce irrational results when disintegrated into finer time scales (i.e., seasonal, monthly), due to their calculation method. For example, for the consecutive dry days, the count can start from 29 July and end by 15 August; in this case, counting the consecutive dry days (CDD) per month, or per season, can lead to ambiguous CDD index, and may invalidate the true description of the index.

Table 2. Summary of all 17 ETCCDI climate indices analyzed in this study, grouped according to its classification.

Index Classification	No.	Climate Index	ID	Threshold Description	Units
Cold duration	1	Frost nighttime [†]	FD	Number of days when $T_{\min} < 0\text{ }^{\circ}\text{C}$	days
	2	Frost daytime [†]	ID	Number of days when $T_{\max} < 0\text{ }^{\circ}\text{C}$	days
Heat duration	3	Summer daytime [†]	SU	Number of days when $T_{\max} > 25\text{ }^{\circ}\text{C}$	days
	4	Summer nighttime [†]	TR	Number of days when $T_{\min} > 20\text{ }^{\circ}\text{C}$	days
Intensity indices— Temperature	5	Coldest nighttime temperature [†]	TNn	Monthly minimum value of daily minimum temp	$^{\circ}\text{C}$
	6	Warmest nighttime temperature [†]	TNx	Monthly maximum value of daily minimum temp	$^{\circ}\text{C}$
	7	Coldest daytime temperature [†]	TXn	Monthly minimum value of daily maximum temp	$^{\circ}\text{C}$
	8	Warmest daytime temperature [†]	TXx	Monthly maximum value of daily maximum temp	$^{\circ}\text{C}$
	9	Diurnal temperature range	DTR	Monthly mean difference between T_{\max} and T_{\min}	$^{\circ}\text{C}$
Intensity indices— Precipitation	10	Max 1-day precipitation depth	RX1day	Maximum 1-day precipitation	mm
	11	Max 5-day precipitation depth *	RX5 day	Maximum consecutive 5-days precipitation	mm
	12	Simple daily intensity index *	SDII	Annual total precipitation divided by the number of wet days	mm/day
	13	Total wet-day precipitation	PRCPTOT	Total precipitation in wet days $\text{PCP} \geq 1\text{ mm}$	mm
Frequency indices— Precipitation	14	Days with heavy precipitation	R10	Number of days when $\text{PRCP} \geq 10\text{ mm}$	days
	15	Days with very heavy precipitation	R20	Number of days when $\text{PRCP} \geq 20\text{ mm}$	days
Duration indices— Precipitation	16	Consecutive dry days *	CDD	Maximum number of consecutive days with $\text{PCP} < 1\text{ mm}$	days
	17	Consecutive wet days *	CWD	Maximum number of consecutive days with $\text{PCP} \geq 1\text{ mm}$	days

* Results were analyzed only on an annual scale. [†] Original name of the climate index was modified to accurately represent the description of the climate index.

To help interpret the results from several indices in an orderly manner, each index was assigned to different classifications, and are summarized in Table 2. Some of the index classifications (i.e., precipitation intensity, precipitation frequency, and frequency duration) used in this study were adapted from the classifications previously presented by Quan et al. [23].

For the calculation of the ETCCDI indices, ETCCDI provides two options to calculate for the annual extreme climate indices: through the use of the (1) ClimDex, a simple Microsoft Excel spreadsheet; or through the (2) RClimDex [31], an R package with a graphical user interface. Both options are provided at the ETCCDI website (<http://etccdi.pacificclimate.org/software.shtml>, accessed on June 2021) available for download. These software are open-source software, however, it only calculates for annual trends. To overcome this challenge, a custom Python code was used to calculate for the extreme climate indices based on different temporal scales (annual, seasonal, and monthly), using daily precipitation, daily minimum, and daily maximum temperatures as input data.

2.3. Trend Analysis

Trend analysis is necessary to determine the presence of significant trends in a climate index, and to quantify the magnitude of trends in a dataset. The trends in datasets can either be monotonic, where a variable consistently increases or decreases through time, or a step trend, where abrupt changes in data may occur at a specific time. Various studies on trend analysis of climate parameters [11–13,15–19,21–23], used the two non-parametric tests known as the Mann–Kendall trend test, and Theil–Sen slope test, to detect significant trends, and to quantify the magnitude of trends, respectively.

2.3.1. Trend-Free Pre-Whitening (TFPW) Method

Prior to performing trend analysis, the time series were checked for the presence of serial correlation. Analyzing time series with existing positive serial correlation can increase the probability of detecting significant trends when there should be none (i.e., Type I error) [32]. Thus, von Storch [32] proposed the use of pre-whitening method to eliminate the serial correlation in time series. Among the several variations of pre-whitening, the TFPW [33], which has been widely used by researchers in the field of hydrometeorology [23,29,30,34,35], was used in this study.

Wu et al. [34] briefly summarized the procedures of TFPW, as follows: (1) The slope of the time series is first estimated using the Theil–Sen slope method, before detrending the time series; (2) the Lag-1 serial correlation coefficient is calculated for the detrended time series, and the AR (1) is eliminated from the detrended series. The resulting residual time series is now an independent time series; (3) the previously determined slope is integrated with the residual time series. The resulting combined time series possesses the real trend of the time series without the AR (1) influence; and lastly (4) the resulting combined time series can now be checked for trends using the Mann–Kendall trend test.

2.3.2. Mann–Kendall (MK) Trend Test

In this study, the Mann–Kendall trend test [24–26], or MK test, was used to detect the presence of significant trends in the selected time series of the selected climate variables. The MK test is a non-parametric test, which does not require the time series data to be linear, nor to be normally distributed. Furthermore, the MK test can detect the presence of monotonic upward or downward trends in a time series. Hirsch et al. [36], defined the MK statistic (S) as:

$$S = \sum_{i=1}^{n-1} \sum_{j=i+1}^n \text{sgn}(x_j - x_i) \quad (1)$$

$$\text{sgn}(x_j - x_i) = \begin{cases} +1 & \text{if } (x_j - x_i) > 0 \\ 0 & \text{if } (x_j - x_i) = 0 \\ -1 & \text{if } (x_j - x_i) < 0 \end{cases} \quad (2)$$

where the x_j , and x_i , are the j th, and i th terms, respectively, in the time series of size n . Equation (2) calculates the number of positive differences minus the number of negative differences. Thus, a positive S , suggests that the most recent data is larger than the previous

data, thus, having an upward trend, while a negative S suggests the contrary. For $n \geq 10$, the average E , and variance (Var) of S are given as shown in Equations (3) and (4).

$$E(S) = 0 \quad (3)$$

where the mean is 0, since Kendall [25] already proved that S is asymptomatic and normally distributed for time series with $n \geq 10$.

$$Var(S) = \frac{1}{18} \left[n(n-1)(2n+5) - \sum_{i=1}^t t_i(t_i-1)(2t_i+5) \right] \quad (4)$$

where t is the number of tied groups in the time series, and t_i is the amount of data in the i th tied group. The statistics of standard test (Z) can be calculated as follows:

$$Z = \begin{cases} \frac{S-1}{\sqrt{Var(S)}} & \text{if } S > 0 \\ 0 & \text{if } S = 0 \\ \frac{S+1}{\sqrt{Var(S)}} & \text{if } S < 0 \end{cases} \quad (5)$$

where Z is used to evaluate the significance of the trend by testing the null hypothesis (H_0). For the Mann–Kendall trend test, the H_0 assumes that there is no monotonic trend in the data, and the alternative hypothesis (H_a) implies that a trend exists in the time series. If the $|Z| > Z_{1-\alpha/2}$, H_0 is rejected and H_a is accepted, thus, implying that the trend is significant at the chosen significance level (α). Based on the two-tailed test, the values of Z for significance levels 5% and 10% are ± 1.96 and ± 1.645 , respectively. For example, if the value of Z falls between the range of ± 1.96 , H_0 is accepted, thus, implying that the trend is non-significant. However, if $|Z| > 1.96$, then H_0 is rejected, and thus implying that the trend is significant at $\alpha = 0.05$. A positive sign of Z indicates an upward trend, and a negative sign for downward trend.

2.3.3. Theil–Sen Slope (TS) Estimator

The Theil–Sen slope estimator is a non-parametric method used to estimate the median of all slopes from a point to its succeeding point, when a linear trend is present in the data. This method requires the time series to have equal intervals, and is resistant or robust to outliers in a time series [37]. The magnitude of the trend is given as:

$$\beta = \text{median} \left(\frac{x_j - x_i}{j - i} \right) \quad \text{where } i < j \quad (6)$$

where β is the median of all slopes between points measured in the i th and j th times. A positive (negative) value of β implies an upward (downward) trend.

2.3.4. Mann–Whitney–Pettit (MWP) Test

The Mann–Whitney–Pettit test [38] was used in this study to detect the most probable change-point in a time series. The MPW test has been widely used in the field of hydrometeorology [39–43], to detect the point where abrupt changes in a time series occurs. The index U_t is given as [44,45]:

$$U_t = \sum_{i=1}^t \sum_{j=i+1}^n \text{sgn}(x_i - x_j) \quad (7)$$

where the x_j , and x_i , are the j th, and i th terms, respectively, in the time series of size n . Additionally, t corresponds to the time where change point occurs. The significant change point is determined where the $|U_t|$ is at its maximum, at time t .

$$K_T = \max_{1 \leq t \leq T} |U_t| \quad (8)$$

$$p(t) = 1 - \exp \left[\frac{-6K_T^2}{n^3 + n^2} \right] \quad (9)$$

where $p(t)$ is the estimated significant probability for a change point [38]; which becomes statistically significant, at significance level of α , when $p(t)$ exceeds $(1 - \alpha)$.

2.3.5. Pearson's Correlation Coefficient

In this study, the Pearson's correlation coefficient (PCC) has been used to investigate significant correlations between the trend magnitudes of the annual climate indices in the UGRB. Previous researchers [46,47] have also utilized the PCC, to create correlation matrices, to investigate the correlations between several climate indices.

3. Results

3.1. Annual Trends

The summary of annual trend magnitudes of the temperature and precipitation indices in the UGRB are summarized in Tables A1 and A2, respectively.

3.1.1. Precipitation

The magnitude of annual trends of both precipitation (left column) and temperature (right column) indices are visually summarized through dot plots shown in Figure A1.

Based on the results of annual trends in precipitation indices, a weak increasing trend for all climate stations was observed for both R10, CDD, and CWD. Both Jeonju, and Jangsu stations in particular were observed to have significant increasing trends in CDD and CWD indices, respectively. These results may suggest that the annual number of days with heavy precipitation, days with prolonged dry, and wet periods, has been generally increasing, as compared from the past.

Furthermore, based on the annual trend results of precipitation intensity indices, the maximum daily intensity, that for all stations, except Jeonju station, has been observed with weak increasing trends. Moreover, the magnitude of trends of the RX1 day index was observed to be significantly correlated with station elevations at 0.89 ($p < 0.05$). Furthermore, the maximum consecutive 5-day intensity at Jeonju and Geumsan stations, were observed with significant increasing trends.

Another notable finding was observed in the overall precipitation indices at Jangsu station, where it exhibits extreme trends for all seven precipitation indices: highest trends on R10, R20, RX1DAY, PRCPTOT, SDII, and CWD, and the lowest RX5DAY. Based on these findings, among all five stations, Jangsu station has been experiencing the most extreme annual precipitation patterns. However, among the precipitation indices, only the RX1Day and CWD indices were observed with significant correlations with station elevations at 0.89 ($p < 0.05$) and 0.86 ($p < 0.05$), respectively.

3.1.2. Temperature

In terms of temperature indices, all stations have shown consistent patterns for every extreme temperature index. Increasing annual trend magnitudes in six indices (i.e., TNn, TNx, TXx, ID, SU, and TR) have been observed, while decreasing trends were observed on three indices (i.e., DTR, TXx, and FD). While, all indices suggest consistent warming of both minimum and maximum temperatures, a declining TXn may suggest that coldest daytime temperature has been annually declining ($\alpha > 0.10$). Furthermore, among the

annual temperature indices, only the TNn index was observed to be significantly correlated with station elevations at 0.88 ($p = 0.05$).

3.1.3. Change Point Detection in Annual Trends

The results of the MWP test, to detect change points in temperature, and precipitation indices, are summarized in Tables 3 and 4, respectively. Though several number of detected change points in the temperature indices were observed, only one change point was detected in the precipitation index. Furthermore, while there was no consistent year detected from all five stations, the heat duration index TR has been observed with an abrupt increase on year 2003 ($p < 0.05$) at Geumsan, Geochang, and Imsil stations. Furthermore, the other heat duration index SU, has also detected with an abrupt increase in slopes, but for different years.

Table 3. Results of MWP test for change point detection in temperature indices.

Classifications	Indices	Jeonju	Geumsan	Geochang	Imsil	Jangsu
Temperature Intensity	DTR	2014	2001	2009	1993	1992
	TNn	2013	2013	2013	2005	2006
	TNx	2011	2016	2005	2008	2007
	TXn	1997	2008	1997	1997	1995
	TXx	2009	2011	2015	2003	2007
Cold Duration	FD	2014	2001	2005	2013	2005
	ID	2008	2008	2008	2013	2013
Heat Duration	SU	1997	2006	2003	2004	2007
	TR	1997	2003	2003	2003	2009

Bold and underlined (*bold italicized*) formatted values are significant at $\alpha = 0.10$ (*0.05*).

Table 4. Results of MWP test to detect change points in precipitation indices.

Classifications	Indices	Jeonju	Geumsan	Geochang	Imsil	Jangsu
Precipitation Duration	CDD	2003	2009	2000	1992	2002
	CWD	2011	1997	2007	2001	1996
Precipitation Intensity	RX1DAY	2011	1994	1997	1996	1995
	RX5DAY	2002	1995	2009	2001	2011
	PRCPTOT	2012	1996	2007	1996	1996
Precipitation Frequency	SDII	1995	1994	2007	1996	1995
	R10	1991	1996	1997	1995	1997
	R20	2004	1996	2007	2012	1995

Bold and underlined (*bold italicized*) formatted values are significant at $\alpha = 0.10$ (*0.05*).

3.1.4. Correlations between Trend Magnitudes of Extreme Climate Indices

The correlation matrix of annual trend magnitudes of all 17 extreme climate indices (values summarized in Tables A1 and A2) is shown in Figure 2. Based on the results of correlation matrix, both temperature intensity and precipitation duration indices were positively correlated with other index classifications. Furthermore, the heat duration, precipitation frequency, and precipitation intensity indices were correlated with all other indices except for cold duration indices. Lastly, the cold duration indices were only correlated with temperature intensity indices.

	DTR	TNN	TNX	TXN	TXX	FD	ID	SU	TR	R10	R20	RX1	RX5	PTOT	SDII	CDD	CWD	Legend
DTR	1.00	<u>0.80</u>	0.46	0.48	<u>0.77</u>	0.62	-0.25	<u>1.00</u>	0.25	0.36	<u>0.69</u>	0.22	0.30	<u>0.86</u>	<u>0.93</u>	0.31	<u>0.87</u>	-1.00
TNN		1.00	0.50	<u>0.68</u>	0.58	0.35	-0.61	<u>0.85</u>	0.25	0.38	<u>0.68</u>	0.58	-0.31	0.64	<u>0.93</u>	0.25	<u>0.99</u>	-0.80
TNX			1.00	<u>0.96</u>	0.27	-0.24	<u>-0.80</u>	0.45	0.22	-0.46	-0.11	0.41	-0.19	0.10	0.37	-0.15	0.54	-0.60
TXN				1.00	0.31	-0.24	<u>-0.89</u>	0.50	0.27	-0.29	0.05	0.60	-0.41	0.16	0.50	-0.13	<u>0.69</u>	-0.40
TXX					1.00	0.23	0.08	<u>0.78</u>	<u>0.79</u>	0.65	<u>0.82</u>	0.55	0.14	<u>0.94</u>	<u>0.79</u>	-0.30	<u>0.67</u>	-0.20
FD						1.00	0.22	0.60	-0.39	0.35	0.48	-0.48	0.61	0.54	0.52	<u>0.82</u>	0.37	-0.20
ID							1.00	-0.28	0.10	0.42	0.14	-0.43	0.57	0.15	-0.31	-0.12	-0.56	0.00
SU								1.00	0.28	0.40	<u>0.73</u>	0.28	0.22	<u>0.87</u>	<u>0.96</u>	0.29	<u>0.90</u>	0.20
TR									1.00	0.52	0.53	<u>0.79</u>	-0.25	0.55	0.37	<u>-0.81</u>	0.31	0.40
R10										1.00	<u>0.92</u>	0.39	-0.06	<u>0.74</u>	0.57	-0.07	0.39	0.60
R20											1.00	0.47	-0.01	<u>0.91</u>	<u>0.85</u>	0.04	<u>0.71</u>	0.80
RX1												1.00	<u>-0.73</u>	0.35	0.47	-0.60	0.56	1.00
RX5													1.00	0.28	-0.02	0.34	-0.21	0.80
PTOT														1.00	<u>0.88</u>	0.03	<u>0.72</u>	1.00
SDII															1.00	0.22	<u>0.96</u>	0.20
CDD																1.00	0.21	0.40
CWD																	1.00	0.60

Figure 2. The correlation matrix between the annual trend magnitudes of all 17 extreme climate indices during the period of 1988–2020. (Underlined and bold formatted values are significant at 0.10, and underlined, and bold italicized values are significant at 0.05; RX1, RX5, and PTOT corresponds to RX1DAY, RX5DAY, and PRCPTOT indices, respectively).

3.2. Seasonal Trends

The seasonal trend magnitudes during spring, summer, autumn, and winter seasons in the UGRB are summarized in Tables A3–A6, respectively.

3.2.1. Precipitation

The results of seasonal trend analysis for all precipitation indices are shown in Figure 3. Based on the results of trend analysis on precipitation frequency indices, both spring and autumn (summer and winter) seasons were observed with weak increasing (decreasing) trends, which suggests an increase (decrease) in the number of days with heavy to very heavy precipitation. The precipitation frequency index R20 was significantly correlated with elevations during spring and autumn seasons at 0.81 and 0.81 ($p < 0.10$).

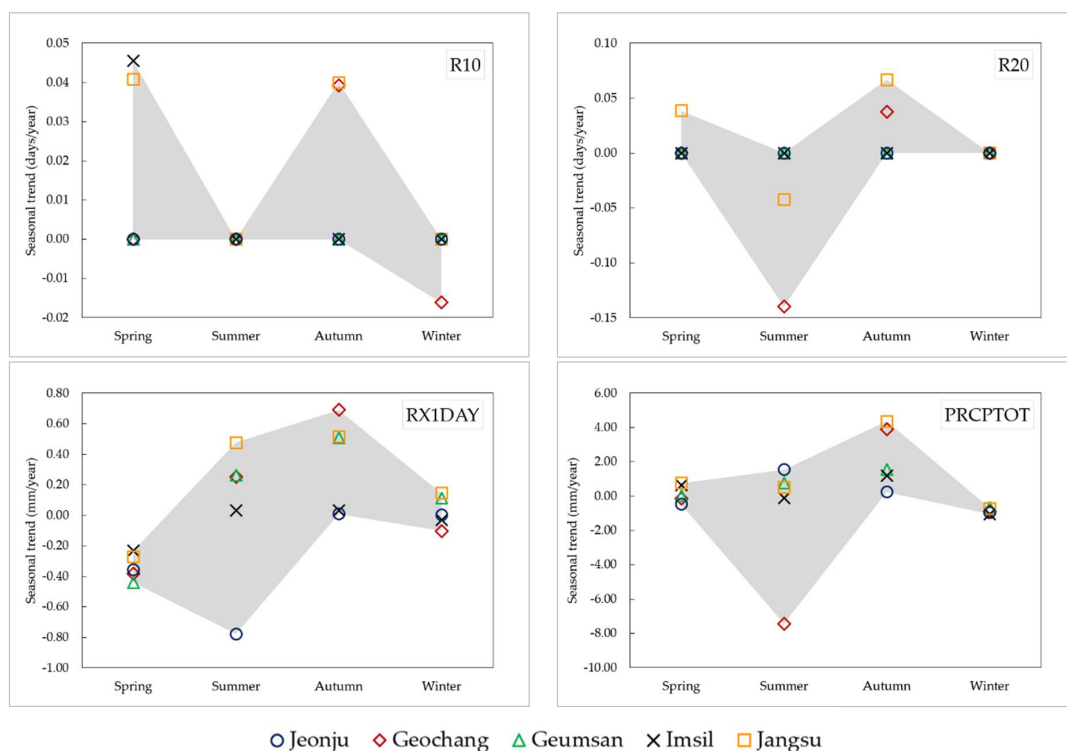


Figure 3. The seasonal trend magnitudes of the precipitation indices at the UGRB.

For the results of the precipitation intensity indices, autumn (winter) season was observed with weak increasing (decreasing) seasonal trend, which suggests that autumn (winter) has been experiencing lesser and weaker daily precipitations. Furthermore, the PRCPTOT index during autumn season showed significant correlation with station elevations. Spring (summer) season was mostly characterized by weak decreasing (increasing) seasonal trends, except for Geumsan (Geochang) station, where a significant decreasing trend was observed for the RX1Day (PRCPTOT) index. These findings suggest that lesser precipitation (weakening daily precipitation intensity) at Geumsan (Geochang) station, during spring (summer) season has been observed. Furthermore, the RX1Day (PRCPTOT) during summer (spring and autumn) season was significantly correlated with station elevations at 0.83 (0.88 and 0.81).

3.2.2. Temperature

The magnitudes of seasonal trends of all temperature intensity indices are shown in Figure 4. It was observed that both spring and summer seasons were mostly characterized by increasing trends, which suggest a global increase in temperature indices at the UGRB. During spring (summer) season, the TXx (TXn) index was observed with the highest magnitude of seasonal trend ($\alpha = 0.05$); which suggests that during spring (summer) season, the warmest daytime (coldest daytime) temperature has been annually increasing.

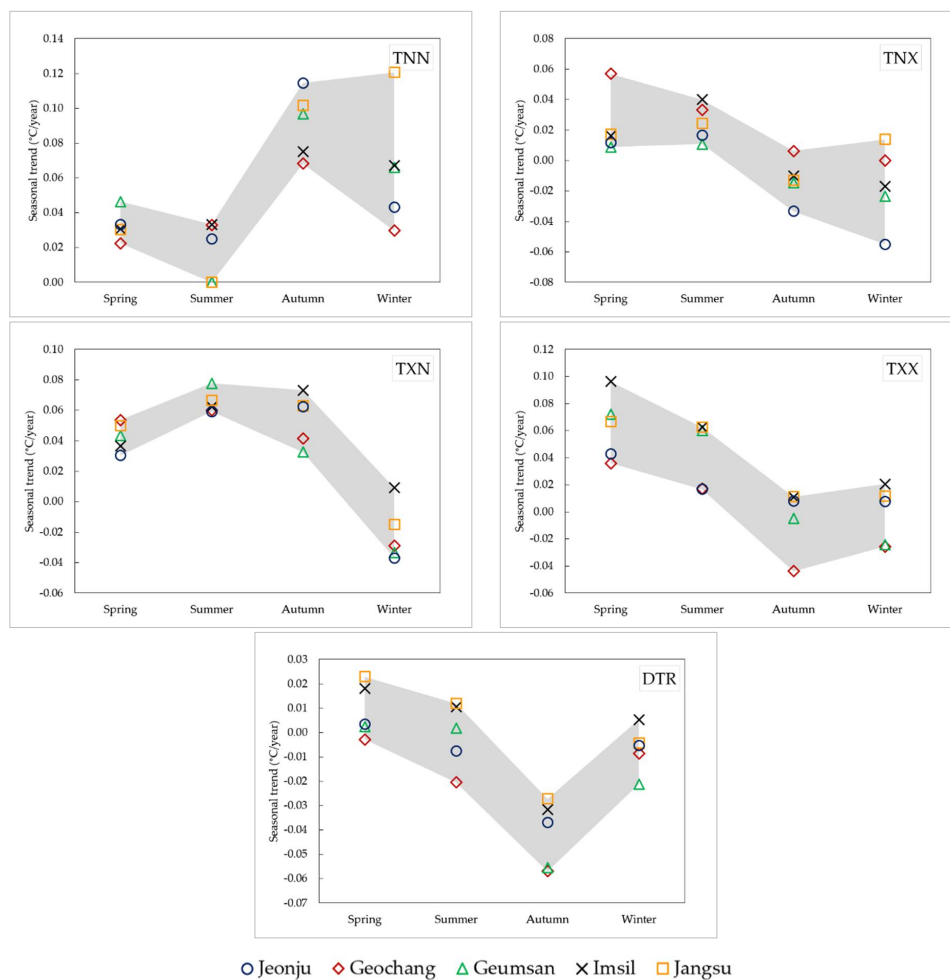


Figure 4. The seasonal trend magnitudes of all temperature intensity indices at the UGRB.

For autumn season, the DTR, TNx, and TXx (TNn and TXn) indices were observed with decreasing (increasing) trends. While DTR and TNn were observed with significant decreasing (increasing) trends, other indices only showed weak seasonal trends. Based

from these findings, the warmest and coldest daytime and nighttime temperatures have been annually decreasing, and increasing, respectively. The decreasing DTR suggests that the temperature gap between daytime and nighttime temperatures has been decreasing annually for autumn season.

For winter season, the temperature intensity indices were observed with weak decreasing trends, except for the TNn index, which was observed with weak and significant increasing trends for all stations. Based on these finding, it can be suggested that winter season has been observed with warming (cooling) of coldest nighttime temperatures (all other temperatures). Furthermore, the TNx index was observed to be significantly correlated with station elevations at 0.93 ($p < 0.05$).

The seasonal trends magnitudes of heat and cold duration indices in the UGRB are shown in Figure 5. Based on the results of cold duration indices, a decreasing (increasing) trend was observed in the FD (ID) index during spring and autumn (winter) seasons. The findings may suggest that the frequency of frost nighttime (daytimes) has been annually decreasing (increasing) during winter season. Furthermore, for the heat duration indices, the results show that both spring and summer (autumn) seasons were observed with significant (weak) increasing trends. Based on these findings, it may be inferred that the frequency of summer daytime and nighttime has been increasing for the past 33 years.

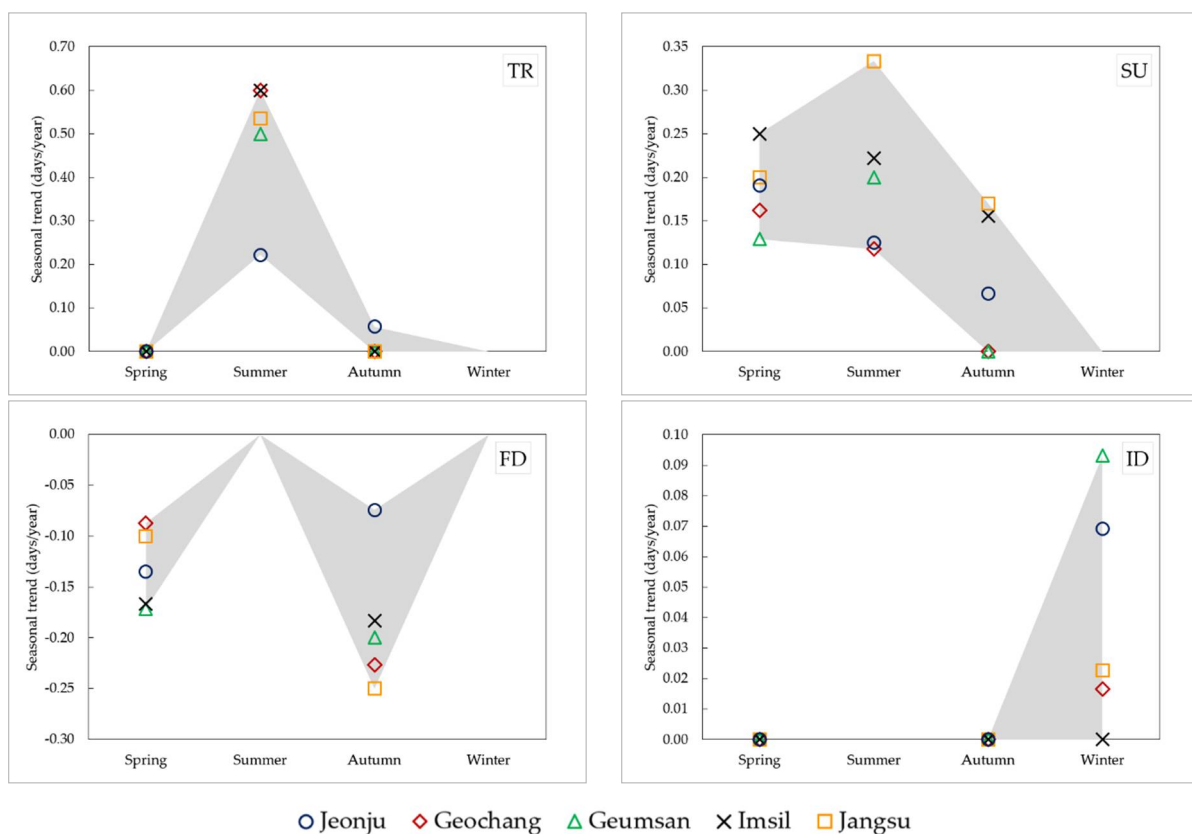


Figure 5. The seasonal trend magnitudes of heat and cold duration indices at the UGRB.

3.3. Monthly Trends

The monthly trend magnitudes from January to December are summarized in Tables A7–A18.

3.3.1. Precipitation

The results of monthly trend analysis of all precipitation indices at the UGRB are shown in Figure 6. Based on the trend results of precipitation frequency indices, the month of June (April, July, October) was observed with decreasing (increasing) trends in

R10 and R20 indices; which suggests that the UGRB has been experiencing an increasing (decreasing) frequency of events with heavy-to-heavy precipitation the month of June (July, October). Moreover, a weak increasing trend in the R10 index during August has been observed; which suggests an increased frequency of events with heavy precipitation has been observed for the last 33 years, at the UGRB. Furthermore, it was also observed that there was no change in trends in the precipitation frequency indices at Jeonju station. Based on these findings, it can be inferred that Jeonju station has been experiencing no changes in precipitation frequency patterns.

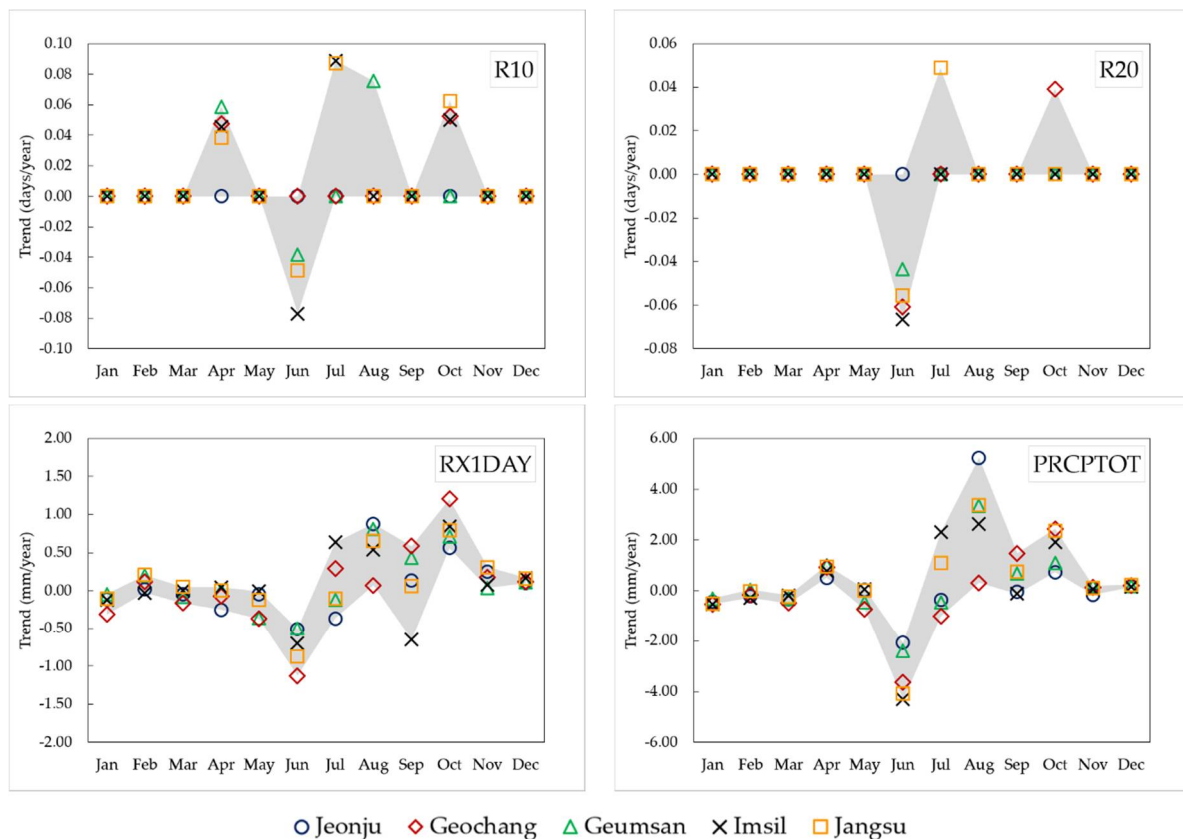


Figure 6. The monthly trend magnitudes of all precipitation indices at the UGRB.

Furthermore, the results from the precipitation intensity indices shows that a big decrease (increase) in the trend magnitude in June (July, August, and October) has been observed. These findings may suggest that the UGRB has been experiencing lower (higher) daily precipitation intensities, and lesser (more) monthly precipitations for the month of June (July, August, and October), for the past 33 years. These findings may suggest precipitation shifts from the month of June, to months of July, August, and October.

3.3.2. Temperature

The monthly trend magnitudes of all five temperature intensity indices are shown in Figure 7. The TNn index has been observed with increasing trends for all months in all stations except for Jangsu station in April and June. These findings may suggest that the coldest nighttime temperature for each month, has been warming since 1988. Furthermore, the TNx index was also observed with consistent increasing trends for all months, except in April, and September, which suggests that the warmest nighttime temperatures during April and September, has been getting colder, while the remaining months have been having warmer nighttime temperatures as compared from 33 years ago.

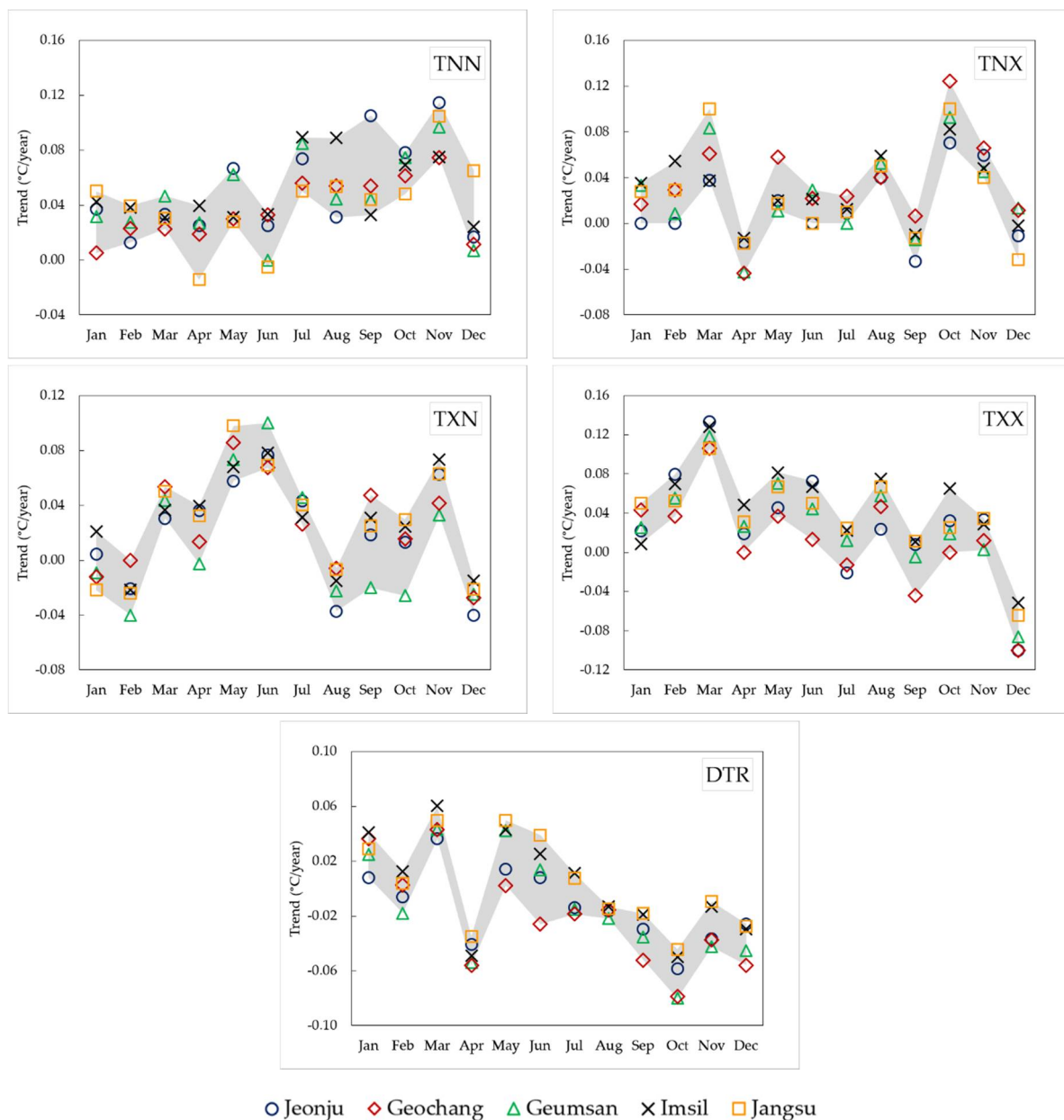


Figure 7. The monthly trend magnitudes of all temperature intensity indices at the UGRB.

Furthermore, during March to July, and November (February, August, and December), the results show an increasing (decreasing) trend in the TXn index, which suggests that the coldest daytime temperatures has been warming (getting colder) for the last three decades. Moreover, the TXx index shows an increasing trend for all months, except for December; which suggests that the warmest daytime temperature in the UGRB has been getting colder, while the rest of the months has been warming.

Finally, based on the results of the DTR index, January, March, May, and June has been observed with increasing trends, which suggests that the temperature gap between the maximum and minimum daily temperatures, for the aforementioned months, has been increasing. Among the aforementioned months, March, May, and June, in particular, were observed with increasing trends for all the remaining temperature indices, beside DTR itself, namely, TNn, TNx, TXn, and TXX. Based on these results, the overall temperature intensity during March, May, and June, has been warming for the past three decades.

The results of monthly trend magnitudes of both heat and cold duration indices are shown in Figure 8. Based on the results of the FD index, decreasing trends were observed during March, April, October, and November, with the latter having the highest magnitude. These results suggest that the frequency of frost nighttime has been decreasing, especially during November, due to the warming of minimum temperature. The ID index on the other hand, was only observed with an increasing trend at Jangsu station during December, suggesting an increase in coldest daytime temperatures at Jangsu station.

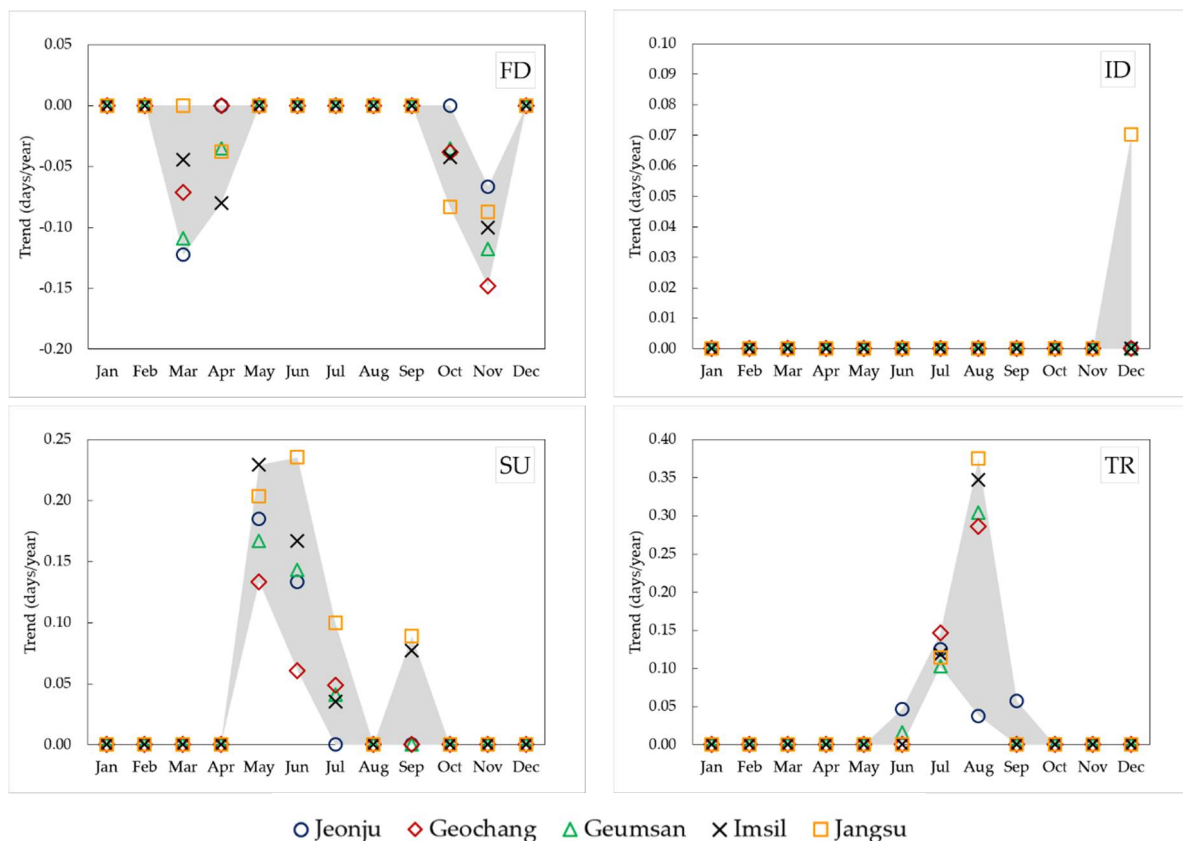


Figure 8. The monthly trend magnitudes of both heat and cold duration indices at the UGRB.

Based on the results of the heat duration index SU, an abrupt change in trend magnitude was observed from May to July, and September (at Jangsu and Imsil stations only); which suggests that the last month of Spring (i.e., May) has been warming up for the past three decades, and months of June and July has been increasing at an abrupt trend, especially at Jangsu station. Furthermore, the TR index has been detected with increasing trends from June to September, which suggests that the aforementioned months have been experiencing an increased frequency of summer nights. These findings suggest a prolonging summer, and thus, a decreasing period of spring, and autumn seasons.

4. Discussion

4.1. Importance of Performing Trend Analysis Based on Detailed Temporal Scales

Based on the results presented in this study, the analysis of trends based on different temporal scales, can provide a more comprehensive understanding of the climate conditions in the UGRB. trend (i.e., May, June, July, and September)

In terms of the heat duration index SU, the high magnitude of annual trend can be misleading as it can be distributed in several seasons (spring, summer, and autumn), and for each season, it can be further disintegrated into the months. Thus, the analysis of monthly trends can specifically help researchers in determining which particular months were observed with increasing or decreasing trends. The findings derived from the monthly

trends have presented relevant results to identify the shortening of spring and autumn seasons, and the prolonged summer season.

Furthermore, in terms of the precipitation intensity index PRCPTOT, a precipitation shift has been determined based on the results of monthly trends (i.e., decreasing trends from January to June, and increasing trends from July to October). Previous researches, presented by Azam et al. [30] and Jung et al. [18], have also determined precipitation shifts, based on the results of monthly trend analysis. In year 2005, Jung et al. [18] previously confirmed that, before 1990s, Jangma season caused heavy precipitation patterns from mid-June to July, however, it started to shift and extend to July to September. More than a decade after, in year 2018, the study of Azam et al. [30] supported the previous findings of Jung et al. [18], and added that decreasing trends were observed from January to June). However, minimal discrepancies (i.e., magnitude of trends) between the presented results from this study, with the findings presented by both Jung et al. [18] and Azam et al. [30] has also been observed; these discrepancies can be attributed to the different methodologies used by researchers (i.e., period of data used in the analysis, climate stations used in the analysis, and utilization of pre-whitening method).

4.2. Effects of Global Warming in the UGRB for the Past Three Decades

The results presented in this study suggests an overall warming of climate conditions in the UGRB, as compared to its previous condition three decades before. In particular, the results based on temperature intensity indices, hot duration indices, and cold duration indices, all suggest an increasing trend in the minimum and maximum temperatures in the UGRB. Furthermore, spring, summer, and autumn seasons, in particular, were greatly affected by global warming. Summer season has become more warmer, and as a result, summer precipitation has also been drier. Zhao and Khalil [48] also observed the same phenomena in the United States, and attributed these findings with climate change. Similarly, the decreasing DTR, also an important indicator of climate change, has been rapidly decreasing during autumn season in the UGRB. These findings were also observed by Qu et al. [49] in the United States. While all seasons except winter season has been warming for the past three decades, the winter season on the contrary has been experiencing colder winters. Similar to the findings of Kug et al. [50], countries in the East Asia, and Northern America has been experiencing an increased frequency of extreme weathers for the past few years, as a result of Arctic warming. These cold events concurrently occurring with Arctic warming and melting of sea ice, which are termed “Warm Arctic, Cold Continent” (WACC), have been attributed to anthropogenic global warming [51].

With proved findings on the effects of anthropogenic global warming in the UGRB, some insights in the future condition of the UGRB can be inferred as follows. Furthermore, Dosio et al. [52] also provided insights on what to expect, in general, from an increase of 0.5 °C to 2.0 °C in the air temperature. Dosio et al. [52] incorporated the ETCCDI indices with the following insights: a decrease in the FD and ID indices can lead to probable impacts in both ecosystem and agriculture, and a surge in agricultural pests, while an increase in the FD and TR indices can cause potential adverse effects on public health.

4.3. Correlation between Elevation and Annual/Seasonal Trend Magnitudes

Based on the results of this study, the three annual indices TN_n, RX1Day, and CWD; and seasonal indices R20 (spring and autumn), RX1Day (summer), PRCPTOT (spring and autumn), and TN_x (winter) were observed with significant positive correlation with the station elevations. Similarly, Awasthi [53] also investigated the correlation between trend magnitudes and station altitudes in Nepal; and have concluded that PRCPTOT, R20 and TN_x indices were negatively correlated with the station elevations and TN_n and CWD, were positively correlated with the station elevations in Nepal. While, some inconsistencies between the result presented by Awasthi, with the results presented in this study can be observed, different temporal scales were used in the analyses. Awasthi [53] utilized annual

trend magnitudes, while this study used both annual and seasonal trend magnitudes. Therefore, based on the results presented in both studies, it can be inferred that the correlation between the annual trend magnitudes of the TNn, RX1Day, and CWD indices, and station elevations, are positively correlated. The difference in magnitudes may be attributed to the different sample sizes, trend analysis methodology, and geographical location.

5. Conclusions

In this study, the recent effects of climate variation in the UGRB have been investigated through a detailed trend analysis of 17 extreme climate indices in the UGRB, based on daily precipitation, daily minimum temperature, and daily maximum temperature data for the past 33 years (1988–2020). Two non-parametric methods, Mann–Kendall trend test, and Theil–Sen slope estimator has been applied in this study, to detect and quantify the magnitude of trends, respectively. Moreover, the Mann–Whitney–Pettitt test was also applied to detect abrupt changes in trend of a time series.

The findings presented in this study suggests that, for the past three decades, the UGRB has been experiencing rising temperatures, prolonged wet and dry periods, increased frequency of precipitation events with heavy to very heavy precipitations patterns, decreasing diurnal temperature range, increasing heat durations, and decreasing cold durations. These findings were attributed to the effects of anthropogenic global warming in the UGRB.

Furthermore, the importance of analyzing climate variables in detailed temporal scales (i.e., monthly) has also been investigated in this study. Based on the results of seasonal and monthly trend analysis, evidence of precipitation shifts of Jangma season (i.e., monsoon season), and prolonging summer season were determined in this study.

Moreover, significant correlation between trend magnitudes, of extreme climate (i.e., annual indices of TNn, RX1Day, and CWD; seasonal indices R20 (spring and autumn), RX1Day (summer), PRCPTOT (spring and autumn), and TNx (winter)) indices, and station elevations were also identified in this study.

Verification of the significant correlation between trend magnitudes and station elevations, should be further investigated on larger catchments, with larger climate station network. Furthermore, the correlation between trend magnitudes of extreme climate indices with other hydrologic parameters (i.e., discharge) in the UGRB, should be also investigated.

The results provided in this study can be used to characterize the recent vulnerability of the UGRB against recent climate conditions.

Author Contributions: Conceptualization, methodology, formal analysis, investigation, data curation, and writing—original draft preparation, M.L.F.; review Y.-k.K., M.C., X.K.D. and T.H.N.; supervision, Y.-k.K., M.C., J.-C.K. and K.J. All authors have read and agreed to the published version of the manuscript.

Funding: This research was supported and funded by the National Research Foundation of Korea, 2019K1A3A1A05087901.

Institutional Review Board Statement: Not applicable.

Informed Consent Statement: Not applicable.

Data Availability Statement: The daily precipitation, daily minimum temperature, and daily maximum temperature used in this study has been obtained from the Korea Meteorological Agency database accessible after login at <https://data.kma.go.kr/> (accessed on June 2020).

Conflicts of Interest: The authors declare no conflict of interest. The funders had no role in the design of the study; in the collection, analyses, or interpretation of data; in the writing of the manuscript, or in the decision to publish the results.

Appendix A. Annual Trends

Table A1. Summary of annual trend magnitudes of the temperature indices in the UGRB for 33 years (1998–2020).

Station Name	Elevation (m.a.s.l.)	Intensity					Cold Duration		Heat Duration	
		DTR	TNN	TNX	TXN	TXX	FD	ID	SU	TR
Jeonju	53.4	-0.01	0.03	0.02	-0.03	0.02	-0.28	0.05	<i>0.46</i>	0.22
Geumsan	170.35	-0.01	0.02	0.01	-0.04	<i>0.06</i>	-0.36	0.12	<i>0.47</i>	<i>0.64</i>
Geochang	225.95	<i>-0.03</i>	0.03	<i>0.03</i>	-0.02	0.02	<i>-0.47</i>	0.00	<i>0.32</i>	<i>0.50</i>
Imsil	247.87	0.00	0.07	<i>0.04</i>	-0.01	<i>0.06</i>	<i>-0.37</i>	0.00	<i>0.66</i>	<i>0.59</i>
Jangsu	406.49	0.00	<i>0.11</i>	<i>0.02</i>	-0.02	<i>0.06</i>	-0.30	0.00	<i>0.71</i>	<i>0.54</i>

Bold underlined (bold italicized) values are significant at $\alpha = 0.10$ (0.05).

Table A2. Summary of annual trend magnitudes of the precipitation indices in the UGRB for 33 years (1998–2020).

Station Name	Elevation (m.a.s.l.)	Frequency			Intensity			Duration	
		R10	R20	RX1DAY	RX5DAY	PRCPTOT	SDII	CDD	CWD
Jeonju	53.4	0.00	-0.04	-0.79	<i>2.82</i>	-0.95	0.00	<i>0.22</i>	0.00
Geumsan	170.35	0.11	0.05	0.25	<i>2.14</i>	2.26	0.01	0.00	0.00
Geochang	225.95	0.00	-0.06	0.67	-1.68	-2.62	-0.01	0.00	0.00
Imsil	247.87	0.00	0.00	0.45	2.00	2.03	0.04	0.04	0.04
Jangsu	406.49	0.11	0.11	0.86	-0.34	3.46	0.06	0.14	<i>0.07</i>

Bold underlined (bold italicized) values are significant at $\alpha = 0.10$ (0.05).



Figure A1. The magnitude of annual trends for both precipitation (left column) and temperature (right column) indices at the UGRB.

Appendix B. Seasonal Trends

Table A3. Trend magnitudes during spring season (MAM) in the UGRB for 33 years (1988–2020).

Station Name	Elevation (m.a.s.l.)	DTR	TNN	Intensity TNX	TXN	TXX	Cold Duration FD	ID	Heat Duration SU	TR	Frequency R10	R20	Intensity RX1DAY	PRCPTOT
Jeonju	53.4	0.00	0.03	0.01	0.03	0.04	−0.13	0.00	0.19	0.00	0.00	0.00	−0.36	−0.48
Geumsan	170.35	0.00	0.05	0.01	0.04	0.07	−0.17	0.00	0.13	0.00	0.00	0.00	−0.44	0.00
Geochang	225.95	0.00	0.02	0.06	0.05	0.04	−0.09	0.00	0.16	0.00	0.00	0.00	−0.38	−0.15
Imsil	247.87	0.02	0.03	0.02	0.04	0.10	−0.17	0.00	0.25	0.00	0.05	0.00	−0.23	0.63
Jangsu	406.49	0.02	0.03	0.02	0.05	0.07	−0.10	0.00	0.20	0.00	0.04	0.04	−0.27	0.76

Bold underlined (bold italicized) values are significant at $\alpha = 0.10$ (0.05).

Table A4. Trend magnitudes during summer season (JJA) in the UGRB for 33 years (1988–2020).

Station Name	Elevation (m.a.s.l.)	DTR	TNN	Intensity TNX	TXN	TXX	Cold Duration FD	ID	Heat Duration SU	TR	Frequency R10	R20	Intensity RX1DAY	PRCPTOT
Jeonju	53.4	−0.01	0.03	0.02	0.06	0.02	-	-	0.13	0.22	0.00	0.00	−0.78	1.54
Geumsan	170.35	0.00	0.00	0.01	0.08	0.06	-	-	0.20	0.50	0.00	0.00	0.26	0.77
Geochang	225.95	−0.02	0.03	0.03	0.06	0.02	-	-	0.12	0.60	0.00	−0.14	0.25	−7.44
Imsil	247.87	0.01	0.03	0.04	0.06	0.06	-	-	0.22	0.60	0.00	0.00	0.03	−0.12
Jangsu	406.49	0.01	0.00	0.02	0.07	0.06	-	-	0.33	0.54	0.00	−0.04	0.48	0.51

Bold underlined (bold italicized) values are significant at $\alpha = 0.10$ (0.05).

Table A5. Trend magnitudes during autumn season (SON) in the UGRB for 33 years (1988–2020).

Station Name	Elevation (m.a.s.l.)	DTR	TNN	Intensity TNX	TXN	TXX	Cold Duration FD	ID	Heat Duration SU	TR	Frequency R10	R20	Intensity RX1DAY	PRCPTOT
Jeonju	53.4	−0.04	0.11	−0.03	0.06	0.01	−0.07	0.00	0.07	0.06	0.00	0.00	0.01	0.25
Geumsan	170.35	−0.06	0.10	−0.01	0.03	−0.01	−0.20	0.00	0.00	0.00	0.00	0.00	0.51	1.55
Geochang	225.95	−0.06	0.07	0.01	0.04	−0.04	−0.23	0.00	0.00	0.00	0.04	0.04	0.69	3.91
Imsil	247.87	−0.03	0.07	−0.01	0.07	0.01	−0.18	0.00	0.16	0.00	0.00	0.00	0.03	1.21
Jangsu	406.49	−0.03	0.10	−0.01	0.06	0.01	−0.25	0.00	0.17	0.00	0.04	0.07	0.52	4.37

Bold underlined (bold italicized) values are significant at $\alpha = 0.10$ (0.05).

Table A6. Trend magnitudes during winter season (SON) in the UGRB for 33 years (1988–2020).

Station Name	Elevation (m.a.s.l.)	DTR	TNN	Intensity TNX	TXN	TXX	Cold Duration FD	ID	Heat Duration SU	TR	Frequency R10	R20	Intensity RX1DAY	PRCPTOT
Jeonju	53.4	−0.01	0.04	−0.06	−0.04	0.01	0.00	0.07	-	-	0.00	0.00	0.00	−0.95
Geumsan	170.35	−0.02	0.07	−0.02	−0.03	−0.02	0.00	0.09	-	-	0.00	0.00	0.11	−0.68
Geochang	225.95	−0.01	0.03	0.00	−0.03	−0.03	0.00	0.02	-	-	−0.02	0.00	−0.10	−0.90
Imsil	247.87	0.01	0.07	−0.02	0.01	0.02	0.00	0.00	-	-	0.00	0.00	−0.03	−1.05
Jangsu	406.49	0.00	0.12	0.01	−0.01	0.01	0.00	0.02	-	-	0.00	0.00	0.14	−0.74

Bold underlined (bold italicized) values are significant at $\alpha = 0.10$ (0.05).

Appendix C. Monthly Trends

Table A7. Trend magnitudes for the month of January in the UGRB for 33 years (1988–2020).

Station Name	Elevation (m.a.s.l.)	DTR	TNN	Intensity TNX	TXN	TXX	Cold Duration FD	ID	Heat Duration SU	TR	Frequency R10	R20	Intensity RX1DAY	PRCPTOT
Jeonju	53.4	0.01	0.04	0.00	0.00	0.02	0.00	0.00	-	-	0.00	0.00	−0.11	−0.44
Geumsan	170.35	0.02	0.03	0.03	−0.01	0.02	0.00	0.00	-	-	0.00	0.00	−0.05	−0.32
Geochang	225.95	0.04	0.01	0.02	−0.01	0.04	0.00	0.00	-	-	0.00	0.00	−0.31	−0.53
Imsil	247.87	0.04	0.04	0.04	0.02	0.01	0.00	0.00	-	-	0.00	0.00	−0.13	−0.54
Jangsu	406.49	0.03	0.05	0.03	−0.02	0.05	0.00	0.00	-	-	0.00	0.00	−0.11	−0.51

Bold underlined (bold italicized) values are significant at $\alpha = 0.10$ (0.05).

Table A8. Trend magnitudes for the month of February in the UGRB for 33 years (1988–2020).

Station Name	Elevation (m.a.s.l.)	DTR	TNN	Intensity TNX	TXN	TXX	Cold Duration FD	ID	Heat Duration SU	TR	Frequency R10	R20	RX1DAY	Intensity PRCPTOT
Jeonju	53.4	−0.01	0.01	0.00	−0.02	0.08	0.00	0.00	-	-	0.00	0.00	0.02	−0.22
Geumsan	170.35	−0.02	0.03	0.01	−0.04	0.06	0.00	(+)0	-	-	0.00	0.00	0.20	0.03
Geochang	225.95	0.00	0.02	0.03	0.00	0.04	0.00	0.00	-	-	0.00	0.00	0.11	−0.16
Imsil	247.87	0.01	0.04	0.05	−0.02	0.07	0.00	0.00	-	-	0.00	0.00	−0.03	−0.29
Jangsu	406.49	0.00	0.04	0.03	−0.02	0.05	0.00	0.00	-	-	0.00	0.00	0.20	−0.03

Bold underlined (bold italicized) values are significant at $\alpha = 0.10$ (0.05).

Table A9. Trend magnitudes for the month of March in the UGRB for 33 years (1988–2020).

Station Name	Elevation (m.a.s.l.)	DTR	TNN	Intensity TNX	TXN	TXX	Cold Duration FD	ID	Heat Duration SU	TR	Frequency R10	R20	RX1DAY	Intensity PRCPTOT
Jeonju	53.4	0.04	0.03	0.04	0.03	0.13	−0.12	-	0.00	-	0.00	0.00	−0.05	−0.36
Geumsan	170.35	0.04	0.05	0.08	0.04	0.12	−0.11	-	0.00	-	0.00	0.00	−0.08	−0.32
Geochang	225.95	0.04	0.02	0.06	0.05	0.11	−0.07	-	0.00	-	0.00	0.00	−0.17	−0.50
Imsil	247.87	0.06	0.03	0.04	0.04	0.13	−0.04	(−)0	0.00	-	0.00	0.00	0.00	−0.19
Jangsu	406.49	0.05	0.03	0.10	0.05	0.11	0.00	0.00	0.00	-	0.00	0.00	0.05	−0.25

Bold underlined (bold italicized) values are significant at $\alpha = 0.10$ (0.05).

Table A10. Trend magnitudes for the month of April in the UGRB for 33 years (1988–2020).

Station Name	Elevation (m.a.s.l.)	DTR	TNN	Intensity TNX	TXN	TXX	Cold Duration FD	ID	Heat Duration SU	TR	Frequency R10	R20	RX1DAY	Intensity PRCPTOT
Jeonju	53.4	− 0.04	0.03	−0.02	0.04	0.02	0.00	-	0.00	-	0.00	0.00	−0.25	0.50
Geumsan	170.35	− 0.05	0.03	−0.04	0.00	0.03	−0.04	-	0.00	-	0.06	0.00	0.00	1.00
Geochang	225.95	− 0.06	0.02	−0.04	0.01	0.00	0.00	-	0.00	-	0.05	0.00	−0.07	0.93
Imsil	247.87	− 0.05	0.04	−0.01	0.04	0.05	−0.08	-	0.00	-	0.05	0.00	0.04	0.78
Jangsu	406.49	−0.03	−0.01	−0.02	0.03	0.03	−0.04	-	0.00	-	0.04	0.00	0.00	0.95

Bold underlined (bold italicized) values are significant at $\alpha = 0.10$ (0.05).

Table A11. Trend magnitudes for the month of May in the UGRB for 33 years (1988–2020).

Station Name	Elevation (m.a.s.l.)	DTR	TNN	Intensity TNX	TXN	TXX	Cold Duration FD	ID	Heat Duration SU	TR	Frequency R10	R20	RX1DAY	Intensity PRCPTOT
Jeonju	53.4	0.01	0.07	0.02	0.06	0.05	-	-	0.18	0.00	0.00	0.00	−0.05	0.03
Geumsan	170.35	0.04	0.06	0.01	0.07	0.07	-	-	0.17	(+)0	0.00	0.00	−0.36	−0.46
Geochang	225.95	0.00	0.03	0.06	0.09	0.04	0.00	-	0.13	(+)0	0.00	0.00	−0.37	−0.75
Imsil	247.87	0.04	0.03	0.02	0.07	0.08	(−)0	-	0.23	(+)0	0.00	0.00	−0.01	0.06
Jangsu	406.49	0.05	0.03	0.02	0.10	0.07	(−)0	-	0.20	(+)0	0.00	0.00	−0.12	0.00

Bold underlined (bold italicized) values are significant at $\alpha = 0.10$ (0.05).

Table A12. Trend magnitudes for the month of June in the UGRB for 33 years (1988–2020).

Station Name	Elevation (m.a.s.l.)	DTR	TNN	Intensity TNX	TXN	TXX	Cold Duration FD	ID	Heat Duration SU	TR	Frequency R10	R20	RX1DAY	Intensity PRCPTOT
Jeonju	53.4	0.01	0.03	0.00	0.08	0.07	-	-	0.13	0.05	0.00	0.00	−0.51	− 2.08
Geumsan	170.35	0.01	0.00	0.03	0.10	0.04	-	-	0.14	0.02	−0.04	− 0.04	−0.50	− 2.41
Geochang	225.95	−0.03	0.03	0.02	0.07	0.01	-	-	0.06	0.00	0.00	− 0.06	− 1.13	− 3.63
Imsil	247.87	0.03	0.03	0.02	0.08	0.07	-	-	0.17	0.00	− 0.08	− 0.07	− 0.70	− 4.31
Jangsu	406.49	0.04	−0.01	0.00	0.07	0.05	-	-	0.24	0.00	−0.05	− 0.06	− 0.87	− 4.07

Bold underlined (bold italicized) values are significant at $\alpha = 0.10$ (0.05).

Table A13. Trend magnitudes for the month of July in the UGRB for 33 years (1988–2020).

Station Name	Elevation (m.a.s.l.)	DTR	TNN	Intensity TNX	TXN	TXX	Cold Duration FD	ID	Heat Duration SU	TR	Frequency R10	R20	RX1DAY	Intensity PRCPTOT
Jeonju	53.4	−0.01	0.07	0.01	0.04	−0.02	-	-	0.00	0.13	0.00	0.00	−0.37	−0.37
Geumsan	170.35	−0.02	0.08	0.00	0.05	0.01	-	-	0.04	0.10	0.00	0.00	−0.13	−0.48
Geochang	225.95	−0.02	0.06	0.02	0.03	−0.01	-	-	0.05	0.15	0.00	0.00	0.29	−1.02
Imsil	247.87	0.01	0.09	0.01	0.03	0.02	-	-	0.04	0.12	0.09	0.00	0.63	2.29
Jangsu	406.49	0.01	0.05	0.01	0.04	0.02	-	-	0.10	0.11	0.09	0.05	−0.10	1.08

Bold underlined (bold italicized) values are significant at $\alpha = 0.10$ (0.05).

Table A14. Trend magnitudes for the month of August in the UGRB for 33 years (1988–2020).

Station Name	Elevation (m.a.s.l.)	DTR	TNN	Intensity TNX	TXN	TXX	Cold Duration FD	ID	Heat Duration SU	TR	Frequency R10	R20	Intensity RX1DAY	PRCPTOT
Jeonju	53.4	−0.02	0.03	0.04	−0.04	0.02	-	-	0.00	0.04	0.00	0.00	0.88	5.23
Geumsan	170.35	−0.02	0.04	0.05	−0.02	0.06	-	-	0.00	0.30	0.08	0.00	0.81	3.34
Geochang	225.95	−0.02	0.05	0.04	−0.01	0.05	-	-	0.00	0.29	0.00	0.00	0.07	0.31
Imsil	247.87	−0.01	0.09	0.06	−0.02	0.08	-	-	0.00	0.35	0.00	0.00	0.53	2.64
Jangsu	406.49	−0.01	0.05	0.05	−0.01	0.07	-	-	0.00	0.38	0.00	0.00	0.65	3.36

Bold underlined (bold italicized) values are significant at $\alpha = 0.10$ (0.05).

Table A15. Trend magnitudes for the month of September in the UGRB for 33 years (1988–2020).

Station Name	Elevation (m.a.s.l.)	DTR	TNN	Intensity TNX	TXN	TXX	Cold Duration FD	ID	Heat Duration SU	TR	Frequency R10	R20	Intensity RX1DAY	PRCPTOT
Jeonju	53.4	−0.03	0.11	−0.03	0.02	0.01	-	-	0.00	0.06	0.00	0.00	0.13	−0.06
Geumsan	170.35	−0.04	0.04	−0.01	−0.02	−0.01	-	-	0.00	0.00	0.00	0.00	0.43	0.67
Geochang	225.95	−0.05	0.05	0.01	0.05	−0.04	-	-	0.00	0.00	0.00	0.00	0.59	1.47
Imsil	247.87	−0.02	0.03	−0.01	0.03	0.01	-	-	0.08	0.00	0.00	0.00	−0.65	−0.13
Jangsu	406.49	−0.02	0.04	−0.01	0.02	0.01	-	-	0.09	0.00	0.00	0.00	0.06	0.73

Bold underlined (bold italicized) values are significant at $\alpha = 0.10$ (0.05).

Table A16. Trend magnitudes for the month of October in the UGRB for 33 years (1988–2020).

Station Name	Elevation (m.a.s.l.)	DTR	TNN	Intensity TNX	TXN	TXX	Cold Duration FD	ID	Heat Duration SU	TR	Frequency R10	R20	Intensity RX1DAY	PRCPTOT
Jeonju	53.4	−0.06	0.08	0.07	0.01	0.03	0.00	-	0.00	0.00	0.00	0.00	0.56	0.72
Geumsan	170.35	−0.08	0.07	0.09	−0.03	0.02	−0.04	-	0.00	-	0.00	0.00	0.71	1.09
Geochang	225.95	−0.08	0.06	0.12	0.02	0.00	−0.04	-	0.00	-	0.05	0.04	1.21	2.43
Imsil	247.87	−0.05	0.07	0.08	0.02	0.06	−0.04	-	0.00	-	0.05	0.00	0.85	1.91
Jangsu	406.49	−0.04	0.05	0.10	0.03	0.02	−0.08	-	0.00	-	0.06	0.00	0.79	2.37

Bold underlined (bold italicized) values are significant at $\alpha = 0.10$ (0.05).

Table A17. Trend magnitudes for the month of November in the UGRB for 33 years (1988–2020).

Station Name	Elevation (m.a.s.l.)	DTR	TNN	Intensity TNX	TXN	TXX	Cold Duration FD	ID	Heat Duration SU	TR	Frequency R10	R20	Intensity RX1DAY	PRCPTOT
Jeonju	53.4	−0.04	0.11	0.06	0.06	0.03	−0.07	-	0.00	-	0.00	0.00	0.25	−0.16
Geumsan	170.35	−0.04	0.10	0.05	0.03	0.00	−0.12	-	0.00	-	0.00	0.00	0.04	0.19
Geochang	225.95	−0.04	0.07	0.07	0.04	0.01	−0.15	-	0.00	-	0.00	0.00	0.17	0.12
Imsil	247.87	−0.01	0.07	0.05	0.07	0.03	−0.10	0.00	0.00	-	0.00	0.00	0.07	0.04
Jangsu	406.49	−0.01	0.10	0.04	0.06	0.03	−0.09	(−)0	-	-	0.00	0.00	0.31	0.09

Bold underlined (bold italicized) values are significant at $\alpha = 0.10$ (0.05).

Table A18. Trend magnitudes for the month of December in the UGRB for 33 years (1988–2020).

Station Name	Elevation (m.a.s.l.)	DTR	TNN	Intensity TNX	TXN	TXX	Cold Duration FD	ID	Heat Duration SU	TR	Frequency R10	R20	Intensity RX1DAY	PRCPTOT
Jeonju	53.4	−0.03	0.02	−0.01	−0.04	−0.10	0.00	0.00	-	-	0.00	0.00	0.10	0.19
Geumsan	170.35	−0.05	0.01	0.01	−0.03	−0.09	0.00	0.00	-	-	0.00	0.00	0.11	0.18
Geochang	225.95	−0.06	0.01	0.01	−0.03	−0.10	0.00	(+) 0	-	-	0.00	0.00	0.12	0.19
Imsil	247.87	−0.03	0.02	0.00	−0.02	−0.05	0.00	0.00	-	-	0.00	0.00	0.17	0.15
Jangsu	406.49	−0.03	0.07	−0.03	−0.02	−0.06	0.00	0.07	-	-	0.00	0.00	0.15	0.23

Bold underlined (bold italicized) values are significant at $\alpha = 0.10$ (0.05).

References

- Donnelly, C.; Greuell, W.; Andersson, J.; Gerten, D.; Pisacane, G.; Roudier, P.; Ludwig, F. Impacts of climate change on European hydrology at 1.5, 2 and 3 degrees mean global warming above preindustrial level. *Clim. Chang.* **2017**, *143*, 13–26. [CrossRef]
- Razavi, T.; Switzman, H.; Arain, A.; Coulibaly, P. Regional climate change trends and uncertainty analysis using extreme indices: A case study of Hamilton, Canada. *Clim. Risk Manag.* **2016**, *13*, 43–63. [CrossRef]
- Intergovernmental Panel on Climate Change (IPCC). *Climate Change 2013: The Physical Science Basis. Contribution of Working Group I to the Fifth Assessment Report of the Intergovernmental Panel on Climate Change*; Stocker, T.F., Qin, D., Plattner, G.-K., Tignor, S.K., Allen, J., Boschung, A., Nauels, Y., Xia, V.B., Midgley, P.M., Eds.; Cambridge University Press: Cambridge, UK, 2013; ISBN 9789291691388.

4. Dinpashoh, Y.; Mirabbasi, R.; Jhahjaria, D.; Abianeh, H.Z.; Mostafaeipour, A. Effect of Short-Term and Long-Term Persistence on Identification of Temporal Trends. *J. Hydrol. Eng.* **2014**, *19*, 617–625. [[CrossRef](#)]
5. Feng, G.; Cobb, S.; Abdo, Z.; Fisher, D.K.; Ouyang, Y.; Adeli, A.; Jenkins, J.N. Trend Analysis and Forecast of Precipitation, Reference Evapotranspiration, and Rainfall Deficit in the Blackland Prairie of Eastern Mississippi. *J. Appl. Meteorol. Climatol.* **2016**, *55*, 1425–1439. [[CrossRef](#)]
6. Sunday, R.K.M.; Masih, I.; Werner, M.; van der Zaag, P. Streamflow forecasting for operational water management in the Incomati River Basin, Southern Africa. *Phys. Chem. Earth Parts A/B/C* **2014**, *72–75*, 1–12. [[CrossRef](#)]
7. Korea Meteorological Agency. *Proven Weather Crisis in Year 2020*; Korea Meteorological Agency: Seoul, Korea, 2021. (In Korean)
8. Moon, J.J.; Kang, S.U.; Lee, J.J. Water for Future. *J. Korea Water Resour. Assoc.* **2020**, *53*, 135–143. (In Korean)
9. Klein Tank, A.M.G.; Zwiers, F.W.; Zhang, X. *Guidelines on Analysis of Extremes in a Changing Climate in Support of Informed Decisions for Adaptation*; World Meteorological Organization: Geneva, Switzerland, 2009.
10. Peterson, T.C.; Manton, M.J. Monitoring Changes in Climate Extreme: A Tale of International Collaboration. *Am. Meteorol. Soc.* **2008**, *89*, 1266–1271. [[CrossRef](#)]
11. Chaney, N.W.; Sheffield, J.; Villarini, G.; Wood, E.F. Development of a High-Resolution Gridded Daily Meteorological Dataset over Sub-Saharan Africa: Spatial Analysis of Trends in Climate Extremes. *J. Clim.* **2014**, *27*, 5815–5835. [[CrossRef](#)]
12. Costa, R.L.; Baptista, G.M.d.M.; Gomes, H.B.; Silva, F.D.d.S.; da Rocha, R.L., Jr.; de Araújo, M.S.; Herdies, D.L. Analysis of climate extremes indices over northeast Brazil from 1961 to 2014. *Weather Clim. Extrem.* **2020**, *28*, 100254. [[CrossRef](#)]
13. Rao, G.V.; Reddy, K.V.; Srinivasan, R.; Sridhar, V.; Umamahesh, N.V.; Pratap, D. Spatio-temporal analysis of rainfall extremes in the flood-prone Nagavali and Vamsadhara Basins in eastern India. *Weather Clim. Extrem.* **2020**, *29*, 100265. [[CrossRef](#)]
14. de los Milagros, M.S.; Brunet, M.; Sigró, J.; Aguilar, E.; Groening, J.A.A.; Bentancur, O.J.; Geier, Y.R.C.; Amaya, R.L.C.; Jácome, H.; Malheiros Ramos, A.; et al. Warming and wetting signals emerging from analysis of changes in climate extreme indices over South America. *Glob. Planet. Chang.* **2013**, *100*, 295–307. [[CrossRef](#)]
15. Wazneh, H.; Arain, M.A.; Coulibaly, P. Historical Spatial and Temporal Climate Trends in Southern Ontario, Canada. *J. Appl. Meteorol. Climatol.* **2017**, *56*, 2767–2787. [[CrossRef](#)]
16. Dietzsch, F.; Andersson, A.; Ziese, M.; Schröder, M.; Raykova, K.; Schamm, K.; Becker, A. A Global ETCCDI-Based Precipitation Climatology from Satellite and Rain Gauge Measurements. *Climate* **2017**, *5*, 9. [[CrossRef](#)]
17. Dong, Z.; Jia, W.; Sarukkalgige, R.; Fu, G.; Meng, Q.; Wang, Q. Innovative Trend Analysis of Air Temperature and Precipitation in the Jinsha River Basin, China. *Water* **2020**, *12*, 3293. [[CrossRef](#)]
18. Jung, I.W.; Bae, D.H.; Kim, G. Recent trends of mean and extreme precipitation in Korea. *Int. J. Climatol.* **2011**, *31*, 359–370. [[CrossRef](#)]
19. Li, X.; Wang, X.; Babovic, V. Analysis of variability and trends of precipitation extremes in Singapore during 1980–2013. *Int. J. Climatol.* **2018**, *38*, 125–141. [[CrossRef](#)]
20. Mahbod, M.; Shirvani, A.; Veronesi, F. A comparative analysis of the precipitation extremes obtained from tropical rainfall-measuring mission satellite and rain gauges datasets over a semiarid region. *Int. J. Climatol.* **2019**, *39*, 495–515. [[CrossRef](#)]
21. N'Tcha M'Po, Y.; Lawin, E.; Yao, B.; Oyerinde, G.; Attogouinon, A.; Afouda, A. Decreasing Past and Mid-Century Rainfall Indices over the Ouémé River Basin, Benin (West Africa). *Climate* **2017**, *5*, 74. [[CrossRef](#)]
22. Nie, H.; Qin, T.; Yang, H.; Chen, J.; He, S.; Lv, Z.; Shen, Z. Trend analysis of temperature and precipitation extremes during winter wheat growth period in the major winter wheat planting area of China. *Atmosphere* **2019**, *10*, 240. [[CrossRef](#)]
23. Quan, N.T.; Khoi, D.N.; Hoan, N.X.; Phung, N.K.; Dang, T.D. Spatiotemporal Trend Analysis of Precipitation Extremes in Ho Chi Minh City, Vietnam During 1980–2017. *Int. J. Disaster Risk Sci.* **2021**, *12*, 131–146. [[CrossRef](#)]
24. Mann, H.B. Nonparametric Tests Against Trend. *Econometrica* **1945**, *13*, 245. [[CrossRef](#)]
25. Kendall, M.G. *Rank Correlation Methods*; Charles Griffin: London, UK, 1975.
26. Gilbert, R.O. *Statistical Methods for Environmental Pollution Monitoring*; Van Nostrand Reinhold Company: New York, NY, USA, 1987; ISBN 0442230508.
27. Theil, H. A Rank-Invariant Method of Linear and Polynomial Regression Analysis. I, II, III. In *Theil's Contributions to Economics and Econometrics. Advanced Studies in Theoretical and Applied Econometrics*; Springer: Amsterdam, The Netherlands, 1950; pp. 345–381.
28. Sen, P.K. Estimates of the Regression Coefficient Based on Kendall's Tau. *J. Am. Stat. Assoc.* **1968**, *63*, 1379–1389. [[CrossRef](#)]
29. Ahmad, I.; Tang, D.; Wang, T.; Wang, M.; Wagan, B. Precipitation Trends over Time Using Mann-Kendall and Spearman's rho Tests in Swat River Basin, Pakistan. *Adv. Meteorol.* **2015**, *2015*, 431860. [[CrossRef](#)]
30. Azam, M.; Maeng, S.; Kim, H.; Lee, S.; Lee, J. Spatial and Temporal Trend Analysis of Precipitation and Drought in South Korea. *Water* **2018**, *10*, 765. [[CrossRef](#)]
31. Zhang, X.; Yang, F. *RClimDex (1.0) User Manual*; Climate Research Branch: Downsview, ON, Canada, 2004; pp. 1–23.
32. Von Storch, H. Misuses of Statistical Analysis in Climate Research. In *Analysis of Climate Variability*; Springer: Berlin/Heidelberg, Germany, 1999; pp. 11–26.
33. Yue, S.; Wang, C.Y. Applicability of prewhitening to eliminate the influence of serial correlation on the Mann-Kendall test. *Water Resour. Res.* **2002**, *38*, 4-1–4-7. [[CrossRef](#)]
34. Wu, H.; Soh, L.-K.; Samal, A.; Chen, X.-H. Trend Analysis of Streamflow Drought Events in Nebraska. *Water Resour. Manag.* **2008**, *22*, 145–164. [[CrossRef](#)]

35. Memarian, H.; Balasundram, S.K.; Talib, J.B.; Sood, A.M.; Abbaspour, K.C. Trend analysis of water discharge and sediment load during the past three decades of development in the Langat basin, Malaysia. *Hydrol. Sci. J.* **2012**, *57*, 1207–1222. [[CrossRef](#)]
36. Hirsch, R.M.; Slack, J.R.; Smith, R.A. Techniques of trend analysis for monthly water quality data. *Water Resour. Res.* **1982**, *18*, 107–121. [[CrossRef](#)]
37. Machiwal, D.; Jha, M.K. *Hydrologic Time Series Analysis: Theory and Practice*, 1st ed.; Springer: Dordrecht, The Netherlands, 2012; ISBN 978-94-007-1860-9.
38. Pettitt, A.N. A Non-Parametric Approach to the Change-Point Problem. *Appl. Stat.* **1979**, *28*, 126. [[CrossRef](#)]
39. Chandniha, S.K.; Meshram, S.G.; Adamowski, J.F.; Meshram, C. Trend analysis of precipitation in Jharkhand State, India. *Theor. Appl. Climatol.* **2017**, *130*, 261–274. [[CrossRef](#)]
40. Hadi, S.J.; Tombul, M. Long-term spatiotemporal trend analysis of precipitation and temperature over Turkey. *Meteorol. Appl.* **2018**, *25*, 445–455. [[CrossRef](#)]
41. Ouhamdouch, S.; Bahir, M. Climate Change Impact on Future Rainfall and Temperature in Semi-arid Areas (Essaouira Basin, Morocco). *Environ. Process.* **2017**, *4*, 975–990. [[CrossRef](#)]
42. Yacoub, E.; Tayfur, G. Trend analysis of temperature and precipitation in Trarza region of Mauritania. *J. Water Clim. Chang.* **2019**, *10*, 484–493. [[CrossRef](#)]
43. Duhan, D.; Pandey, A. Statistical analysis of long term spatial and temporal trends of precipitation during 1901–2002 at Madhya Pradesh, India. *Atmos. Res.* **2013**, *122*, 136–149. [[CrossRef](#)]
44. Chen, S.-T.; Kuo, C.-C.; Yu, P.-S. Historical trends and variability of meteorological droughts in Taiwan/Tendances historiques et variabilité des sécheresses météorologiques à Taiwan. *Hydrol. Sci. J.* **2009**, *54*, 430–441. [[CrossRef](#)]
45. Mondal, A.; Khare, D.; Kundu, S. Spatial and temporal analysis of rainfall and temperature trend of India. *Theor. Appl. Climatol.* **2015**, *122*, 143–158. [[CrossRef](#)]
46. Afzal, M.; Gagnon, A.S.; Mansell, M.G. Changes in the variability and periodicity of precipitation in Scotland. *Theor. Appl. Climatol.* **2015**, *119*, 135–159. [[CrossRef](#)]
47. Yeh, P.J.F.; Wu, C. Recent Acceleration of the Terrestrial Hydrologic Cycle in the U.S. Midwest. *J. Geophys. Res. Atmos.* **2018**, *123*, 2993–3008. [[CrossRef](#)]
48. Zhao, W.; Khalil, M.A.K. The Relationship between Precipitation and Temperature over the Contiguous United States. *J. Clim.* **1993**, *6*, 1232–1236. [[CrossRef](#)]
49. Qu, M.; Wan, J.; Hao, X. Analysis of diurnal air temperature range change in the continental United States. *Weather Clim. Extrem.* **2014**, *4*, 86–95. [[CrossRef](#)]
50. Kug, J.-S.; Jeong, J.-H.; Jang, Y.-S.; Kim, B.-M.; Folland, C.K.; Min, S.-K.; Son, S.-W. Two distinct influences of Arctic warming on cold winters over North America and East Asia. *Nat. Geosci.* **2015**, *8*, 759–762. [[CrossRef](#)]
51. Overland, J.E.; Wood, K.R.; Wang, M. Warm Arctic—Cold continents: Climate impacts of the newly open Arctic Sea. *Polar Res.* **2011**, *30*, 15787. [[CrossRef](#)]
52. Dosio, A. *Mean and Extreme Climate in Europe*; European Commission: Brussels, Belgium, 2020.
53. Awasthi, R.P. Variability of Climate Extremes in Variability of Climate Extremes in Nepal. Master's Thesis, Hankuk University of Foreign Studies, Seoul, Korea, 2018.